Transportation Research Record

Experiments on the influence of wall-shaped obstacle on pedestrian egress efficiency

--Manuscript Draft--

Full Title:	Experiments on the influence of wall-shaped obstacle on pedestrian egress efficiency
Abstract:	Experiments have been conducted to explore the influence of a wall--shaped obstacle on pedestrian flow under non-emergency conditions. Results show that both the obstacle size and obstacle-exit distance could influence the egress efficiency. The increase of obstacle size has no influence on egress efficiency when obstacle-exit distance is small, while would reduce the egress efficiency when obstacle-exit distance is large. For further analysis, we have abstracted the walking scenario into a simple network with the bottlenecks as links and different regions as nodes. It is indicated that when the obstacle-exit distance is smaller, the bottleneck at the obstacle would act as an `ineffective' bottleneck that would not apparently affect the egress time. Nevertheless, when the obstacle-exit distance is larger, the bottleneck at the obstacle would act as an 'effective' bottleneck that would decrease the egress efficiency. It is interesting that the exit bottleneck, though always with the least flow rate, is not always the 'effective' bottleneck. Furthermore, we have built a mathematical model that could be used to estimate the egress time under certain obstacle size and obstacle-exit width. Consequently, a reasonable range of obstacle size and obstacle-exit width, under which condition the egress time is not apparently increased, has been obtained. Results in this study are expected to help in the actual design of obstacles in walking facilities.
Manuscript Classifications:	Operations and Traffic Management; Traffic Flow Theory and Characteristics AHB45; Models; Pedestrians
Manuscript Number:	
Article Type:	Presentation and Publication
Order of Authors:	Xiaolu JIA
	Daichi Yanagisawa
	Claudio Feliciani
	Katsuhiro Nishinari

EXPERIMENTS ON THE INFLUENCE OF WALL–SHAPED OBSTACLE ON PEDESTRIAN EGRESS EFFICIENCY

Xiaolu Jia
Department of Advanced Interdisciplinary Studies, Graduate School of Engineering
The University of Tokyo, 4-6-1, Komaba, Meguro-ku, Tokyo, Japan, 153-8904
Email: xiaolujia@g.ecc.u-tokyo.ac.jp

Daichi Yanagisawa
Research Center for Advanced Science and Technology
The University of Tokyo, 4-6-1, Komaba, Meguro-ku, Tokyo, Japan, 153-8904

Department of Aeronautics and Astronautics, Graduate School of Engineering
The University of Tokyo, 7-3-1 Hongo, Bunkyo-ku, Tokyo, Japan, 113-8656
Email: tDaichi@mail.ecc.u-tokyo.ac.jp

Claudio Feliciani
Research Center for Advanced Science and Technology
The University of Tokyo, Tokyo, Japan, 153-8904
Email: feliciani@jamology.rcast.u-tokyo.ac.jp

Katsuhiro Nishinari
Research Center for Advanced Science and Technology
The University of Tokyo, Tokyo, Japan, 153-8904

Department of Aeronautics and Astronautics, Graduate School of Engineering
The University of Tokyo, 7-3-1 Hongo, Bunkyo-ku, Tokyo, Japan, 113-8656
Email: tknishi@mail.ecc.u-tokyo.ac.jp

Word Count: 5602 words + 3 table(s) $\times$ 250 = 6352 words

Submission Date: August 1, 2019

ABSTRACT

Experiments have been conducted to explore the influence of a wall–shaped obstacle on pedestrian flow under non-emergency conditions. Results show that both the obstacle size and obstacle-exit distance could influence the egress efficiency. The increase of obstacle size has no influence on egress efficiency when obstacle-exit distance is small, while would reduce the egress efficiency when obstacle-exit distance is large. For further analysis, we have abstracted the walking scenario into a simple network with the bottlenecks as links and different regions as nodes. It is indicated that when the obstacle-exit distance is smaller, the bottleneck at the obstacle would act as an 'ineffective' bottleneck that would not apparently affect the egress time. Nevertheless, when the obstacle-exit distance is larger, the bottleneck at the obstacle would act as an 'effective' bottleneck that would decrease the egress efficiency. It is interesting that the exit bottleneck, though always with the least flow rate, is not always the 'effective' bottleneck. Furthermore, we have built a mathematical model that could be used to estimate the egress time under certain obstacle size and obstacle-exit width. Consequently, a reasonable range of obstacle size and obstacle-exit width, under which condition the egress time is not apparently increased, has been obtained. Results in this study are expected to help in the actual design of obstacles in walking facilities.

Keywords: Pedestrian dynamics, Egress efficiency, Obstacle, Effective bottleneck

INTRODUCTION

In walking facilities such as subway stations, sports venues and commercial buildings, pedestrian movement is often affected by obstacles like walls, pillars and interior furnishings. Therefore, exploring the influence of obstacles on pedestrian movement is significant to the actual design of obstacles in order to guarantee a more comfortable and efficient walking environment.

Research on the influence of obstacle began to attract more attention since it was proposed that placing an obstacle before the exit could help improve the evacuation efficiency (*1*). For particles without self–awareness such as grains in silo (*2*), sheep (*3*), ants (*4*) and mice (*5*), the efficiency improvement of obstacle before the exit has been experimentally proved.

In the case of pedestrian flow, agent-based models (a review seen in (*6*)) have been widely used to emulate the influence of obstacle on panic evacuation. Many studies have demonstrated the merits of obstacle before the exit in improving the evacuation efficiency (*7–11*). One of the main reasons for the improvement of evacuation efficiency is that the obstacle could help decrease the conflicts caused by friction and turning behavior of pedestrians before the exit (*7, 8, 12*). Other reasonable obstacle settings that could help improve the evacuation efficiency have also been evaluated (*13, 14*). On the other hand, some studies reminded us that under conditions where pedestrians cannot fully recognize the exit location, the obstacle could have negative effect on evacuation efficiency through obstructing the sights of pedestrians (*15*). However, the lack of experimental evidence for modeling rules might make the simulation results unconvincing. As a result, many experimental studies have been conducted to provide evidence for modeling calibration. For instance, the obstacle–evading behavior of several pedestrians have been experimentally analyzed in (*16–18*) to provide evidence for the collision–avoidance rules of agent-based models.

Different from simulation studies, it is difficult to implement panic or very competitive experiments due to safety and ethical reasons. As a results, most of the experiments have been conducted under normal or slightly competitive situations. Under slow running and corner exit conditions, the obstacle was proved to be more helpful in increasing the evacuation efficiency than the normal walking and middle exit conditions (*19*). It was also proposed that the efficiency would be improved more effectively if the obstacle was shifted from the exit center (*7, 8*). The function of obstacle to reduce conflicts have also been observed in other scenarios such as pedestrian intersection (*20*) where there were more conflicts among pedestrians. Other experiments showed that in relatively panic conditions, placing two obstacles before the exit would contribute to a higher evacuation efficiency compared with one obstacle or no-obstacle case (*14*). On the other hand, some studies proposed that the obstacle only worked well on granular flow but barely worked for actual pedestrians especially in highly crowded and competitive conditions (*21*). Although the pedestrians were already very competitive in their experiments, the obstacle in their experiments could not reduce conflicts.

In most present research, the obstacles were pillar–shaped and only placed before the exit. However, in actual situations, wall–shaped obstacles like partition walls and fences have also been widely applied, and the locations of obstacle is not limited to near the exit. Therefore, a more generalized study on the influence of wall–shaped obstacle on pedestrian egress efficiency should be conducted.

Furthermore, a wall–shaped obstacle could form bottleneck while occupying a much smaller space than a pillar–shaped obstacle. As a result, a double-bottleneck situation where pedestrians are impeded by both the obstacle and exit bottleneck could be constructed. The pedestrian behavior at a single bottleneck have been widely explored at normal bottleneck with a decrease of corridor width (*22–24*) or at the conjunction of T–shaped corridor (*25, 26*). However, there are relatively few studies in the case of multiple bottlenecks. In a simulation study where bottlenecks have been added before the exit (*27*), it is shown that decreasing the flow at the extra bottlenecks would in turn improve the flow at the exit through decreasing the conflicts before the exit. As to the authors knowledge, there is no experimental study on the double-bottleneck situation caused by the obstacle.

Therefore, we would like to conduct experiments to examine the influence of wall–shaped obstacle on pedestrian egress efficiency and analyze the influencing mechanism from the perspective of double-bottleneck condition. Furthermore, based on the experimental results, we would like to build a mathematical model that could estimate the egress time under other obstacle layouts that have not been examined in the experiments.

EXPERIMENT SETUP

Experiments have been performed to explore the influence of obstacle size and location on the egress of crowd pedestrians. The experiments were conducted on December, 2018 in the outdoor open space in front of the RCAST Building 4, The University of Tokyo, Japan. The experiment scenario was set as a corridor with a wall–shaped obstacle placed at the horizontal middle axis.

Totally 49 participants have joined in our experiments. Detailed information of the participants can be seen in Table 1. Among the participants, there were 29 males and 20 females whose age ranged from 18 to 78 years old and height ranged from 145 to 180 cm. All the participants had no walking impairment. Meanwhile, despite some studies showed that cultural difference affects pedestrian behavior(*28*), we would like to ignore the influence of cultural difference because most of our participants were Japanese and the two foreigners had been living in Japan for at least two years. We presume that the diversity of our participants makes our experiments more approximate to real egress cases with high heterogeneity of pedestrians.

TABLE 1 Personal information of participants

age (years)		height (cm)		gender		nationality	
range	average	range	average	male	female	Japanese	Chinese
18−78	46±24	145−180	164.3±8.4	29	20	47	2

FIGURE 1 The geometrical layout of experimental setting

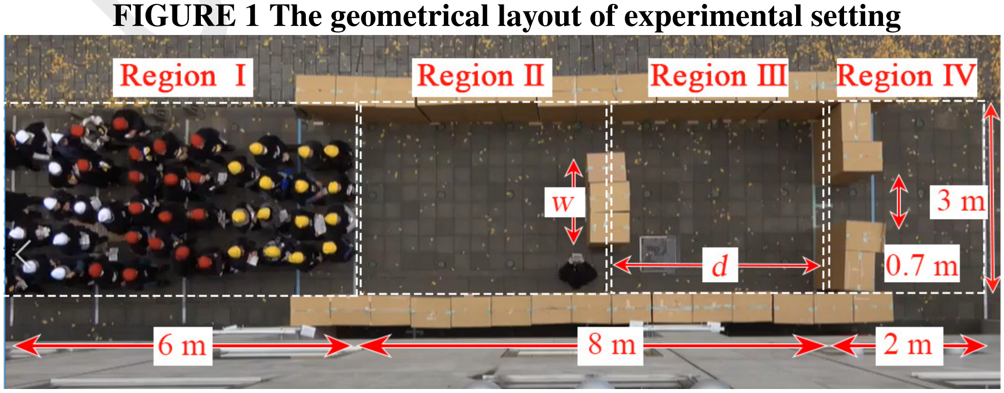

As can be seen in Fig. 1, the whole scenario is divided into Region I, II, III and IV with the dashed lines as borders. Region I is the pedestrian waiting region that provided pedestrians with spaces to stand before each experiment test. Region II and III is respectively the walking region before and after the obstacle. Pedestrians were required to walk straight in Region IV after passing by the exit in order not to impede the pedestrians in the corridor.

The obstacle width w and the obstacle-exit distance d were variable. Considering the obstacle was built by cardboard boxes, we would like to define the number of boxes that were used to build the obstacle as *box*. The width of each box is 0.42 m, and the obstacle width w can be calculated accordingly. The values of *box*, w, d in each test can be seen in Tab. 2. All the experiments have been repeated for at least two times.

TABLE 2 The geometrical conditions of each test

d [m]	*box*	w [m]	repetitions
-	0	0	2
4	1	0.42	2
	2	0.84	2
	3	1.26	2
	4	1.68	2
1	1	0.42	2
	2	0.84	3
	3	1.26	2

Before each experiment test, participants were required to stand randomly in Region I. Afterwards, they were instructed to start walking together, traverse Region II and III in order to egress from the exit, and keep walking straight in Region IV to avoid impeding other pedestrians. A camera was set above the horizontal axis of the corridor and fixed about 20 meters above the ground. Recordings of the camera was adjusted to 4k mode (3840×2160 pixel) with a frame rate of 30 fps. With the videos of the experiments as raw data, the recognition and tracking of pedestrians could be achieved using PeTrack software (*29*). Pedestrians were required to wear colored caps and black shirts so that their positions at each video frame could be detected.

INFLUENCE OF OBSTACLE ON EGRESS EFFICIENCY IN EXPERIMENTS

In this section, we would like to examine the influence of obstacle on the egress efficiency through calculating the egress time. For a certain experiment run, we define t_i^{in} and t_i^{out} respectively as the moment for pedestrian i to get into Region II and leave Region III through the exit. Numbering the 49 pedestrians by the sequence to pass through the exit, we define the egress time T of a certain experiment run as the time for the first 46 pedestrians to traverse Region II and Region III. In other words, the egress time T is equal to the time lag between the first pedestrian steps into Region II and the 46$^{\text{th}}$ pedestrian leaves Region III. Calculation of T can be seen in Equation 1.

$$T = t_j^{\text{out}} - t_i^{\text{in}} \quad (i = 1, \quad j = 46) \tag{1}$$

We do not consider the last three pedestrians because they had no pedestrians behind to affect them and may largely affect the total egress time. The variation of egress time T with obstacle width w under two types of obstacle-exit distance d can be seen in Figure 2. It can be seen from Figure 2 that when $d = 4$ m, the egress time T would roughly rise with the increase of obstacle size. We hence assume that the existence of obstacle would decrease the egress efficiency when $d = 4$ m. By contrast, when $d = 1$ m, the egress time tends to keep constant despite the increase of obstacle size. Therefore, we assume that the existence of obstacle does not affect the egress efficiency when $d = 1$ m. We could hence conclude that the influence of obstacle width on egress time is affected by obstacle-exit distance.

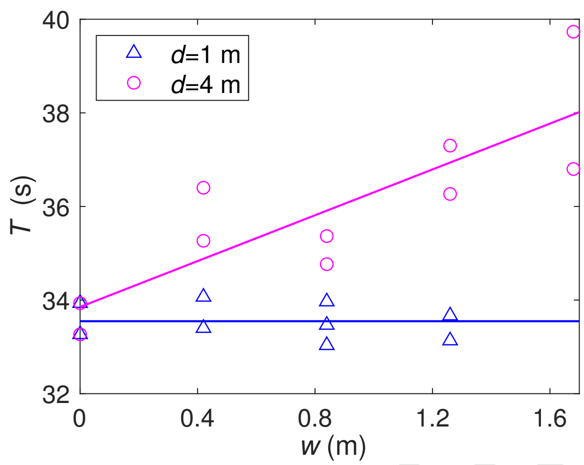

FIGURE 2 Variation of egress time under different obstacle sizes and locations

To explore the influencing mechanism of obstacle-exit distance on pedestrian egress, we would like to abstract the walking scenario in Fig. 1 as a simple network. To be specific, the four regions could be considered as nodes and the bottlenecks considered as links between nodes. The pedestrian number at Region I, Region II, Region III and Region IV are respectively defined as N_1, N_2, N_3 and N_4, and the flow rate, i.e. the number of pedestrians that pass by a section within one second, among different regions are respectively defined as Q_{in}, Q_{obs} and Q_{out}. The network can be illustrated in Equation 2.

$$N_1 \xrightarrow{Q_{in}} N_2 \xrightarrow{Q_{obs}} N_3 \xrightarrow{Q_{\mathrm{out}}} N_4 \tag{2}$$

Together with the bottleneck at the exit, the existence of obstacle makes the walking scenario a double-bottleneck environment. Initially, all the 49 pedestrians were allocated in Region I. Afterwards, pedestrians would move from Region I, pass by Region II and Region III, and finally leave the experimental region after passing by Region IV. With the variation of obstacle size w and obstacle-exit distance d, the Q_{obs} and Q_{out} would also variate, which might be the main reason for the variation of egress time under different conditions. The variation of Q_{obs} and Q_{out} under different w and d in our experiments can be seen in Figure 3.

It can be seen in Fig. 3(a) that the variation trend of Q_{obs} against obstacle width w would change under different obstacle-exit distance d. The dots represent the experimental data and the straight lines are the fitting curves to show the variation trend. It is shown that the Q_{obs} will roughly decrease with the rise of w under $d = 4$ m, and we define its corresponding value as $Q_{\mathrm{obs}}^{\mathrm{max}}$. In contrast, under $d = 1$ m, the Q_{obs} tends to keep constant at certain value despite the increase of

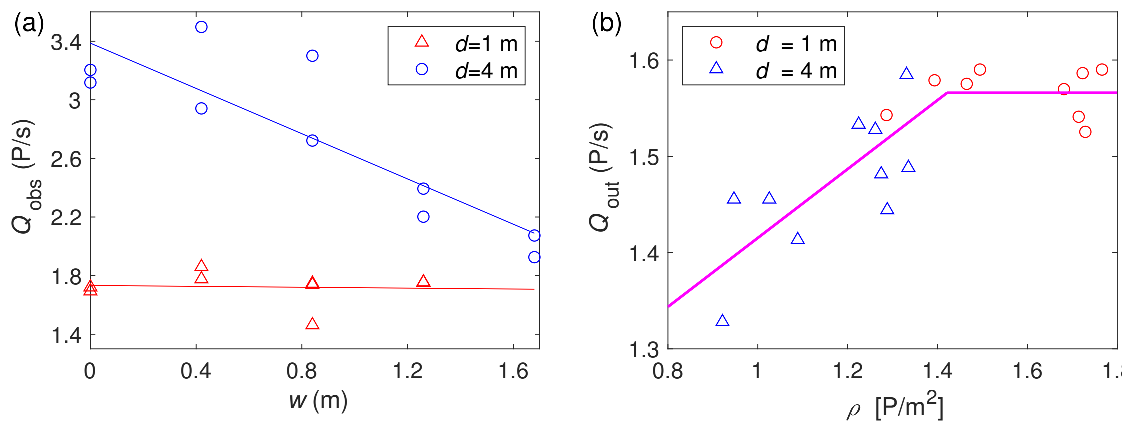

FIGURE 3 Variation of flow rate at the bottlenecks of (a) obstacle and (b) exit.

obstacle width w. The equations of the fitting curves can be seen in Equation 3.

$$Q_{obs} = \begin{cases} Q_{\text{obs}}^{\max} = Aw + B & (d = 4\text{m}) \\ 1.73 & (d = 1\text{m}) \end{cases} \qquad (A = -0.77, \quad B = 3.39) \tag{3}$$

The different variation trends of Q_{obs} could indicate different effects of the obstacle on egress efficiency. As can be seen in Figure 3(a), the Q_{obs} is affected by obstacle size when $d = 4$ m, which means the obstacle forms an 'effective' bottleneck that could obstruct pedestrian flow. By contrast, when $d = 1$ m, the obstacle has no influence on the egress efficiency, which means the obstacle forms an 'ineffective' bottleneck that would not obstruct pedestrian egress.

We presume that the variation of flow rate at the exit could help explain our assumption about the 'ineffective' and 'effective' bottleneck. In Figure 3(b), ρ represents the average pedestrian density at Region III during one whole egress process. The dots are the experimental data showing the relation between ρ and Q_{out}. Through observation, we presume that Q_{out} tends to increase with ρ when $d = 4$ m, while tends to keep constant when $d = 1$ m. Accordingly, a piecewise linear function has been used to fit the dots and illustrated by straight lines in Figure 3(b). The variation of Q_{out} with ρ in the fitting function can be seen in Equation 4.

$$Q_{\text{out}} = \begin{cases} C\rho + D & (\rho < \rho_{\text{cri}}) \\ Q_{\text{out}}^{\max} & (\rho \geq \rho_{\text{cri}}) \end{cases} \qquad (C = 0.35, \quad D = 1.10, \quad Q_{\text{out}}^{\max} = 1.58, \quad \rho_{\text{cri}} = 1.4) \tag{4}$$

It is shown that with the increase of average density ρ, the flow rate at the exit Q_{out} would first gradually increase, and then keep constant after the density reaches $\rho_{cri} = 1.4$ P/m^2. We presume the different increasing trend of egress time under under different obstacle-exit distances could be explained by the variation of density. Under the same inflow rate Q_{obs}, the area of Region III is 12 m^2 when $d = 4$ m and 3 m^2 when $d = 1$ m. Therefore, it would take a longer time to reach the critical density ρ_{cri} under the condition when $d = 4$ m. In other words, the duration when $\rho = \rho_{cri}$ is longer when $d = 1$ m. Since the Q_{out} under $\rho < \rho_{cri}$ is smaller than that when $\rho = \rho_{cri}$, the average Q_{out} under $d = 4$ m is smaller than that under $d = 1$ m.

MODELING THE INFLUENCE OF OBSTACLE ON PEDESTRIAN EGRESS

According to our experimental results, we have discovered that the egress time is affected by both the obstacle width and obstacle-exit width. Based on the analytical results, we would like to build a mathematical model that could reproduce the experimental egress time under different obstacle layouts. With the mathematical model, we could estimate the egress time under a variety of obstacle layouts that are not limited by the obstacle layouts in our experiments. Furthermore, the estimation results of the model is expected to help guiding the actual design of obstacle.

Necessity of building a more complex mathematical model

We would like to first give the most common idea that can be usually thought of when calculating the egress time in the simple network shown in Equation 2, thus indicating the necessity of building a more complex model to reproduce the influence of obstacle layouts.

For a general network with the structure in Equation 2, the outflow time could be calculated through dividing the volume by the flow capacity of the network. One of the basic assumptions of the Minimum-Cost Flow Problem, which has been widely used for static traffic assignment (*30*), indicates that the network capacity is equal to the minimum capacity of all the arrows. In other words, the arrow with the minimum capacity is the only bottleneck that impede the flow. In our experiments, the exit width is 1 m while the least bottleneck width at the obstacle is 1.32 m. Therefore, the exit can be considered as the main bottleneck and the capacity of the network is equal to the capacity of the exit.

In this sense, to estimate the whole egress time of our experimental results, we presume the egress time could be separated into two periods. The first period is from the beginning to the first pedestrian reaches the exit, during which period there will be no outflow at the exit. The second period is from the first pedestrian leaves the corridor to the 46$^{\text{th}}$ pedestrian leaves the corridor. During the second period, pedestrians would consecutively egress from the exit. With the method above, the egress time in our experiments could be estimated as below.

In the first period, the duration is the time it costs for the first pedestrian to reach the exit. We assume the free flow velocity as $v = 1.5$ m/s and the walking distance as 8 m, i.e. the corridor length. The detour distance caused by the obstacle would be ignored because the detour distance would be mostly 0.2 m, which is neglectable compared with the corridor length. Meanwhile, the obstacle would not affect pedestrian velocity under free flow conditions (*18*). As a result, the duration of the first period can be estimated as $8/1.5 = 5.33$ s.

In the second period, the common idea for calculation is to divide the total pedestrian number with flow capacity at the exit. As is shown in Figure 3(b), the flow capacity at the exit is $Q_{\text{out}}^{\text{max}}$ =1.58 P/s. As a result, the duration of the second period, i.e. the time period from the first pedestrian arrive at the exit to the 46$^{\text{th}}$ pedestrian leaves the corridor, can be estimated as $45/1.58 = 28.48$ s. Accordingly, the total egress time can be estimated as the sum of the two periods. The estimated egress time is 33.81 s, which is in accordance with the experimental egress time without obstacle as shown in Figure 2.

Despite this simple calculation could reproduce the egress time when there is no obstacle, the influence of obstacle width on egress time would be neglected because the bottleneck at the obstacle is never the main bottleneck in our experimental scenario. As a result, this simple estimation method could not be used to estimate the influence of obstacle.

We presume the main reason that causes the inaccordance of estimation results with the experimental results is the assumption in the Minimum-Cost Flow Problem that the capacity of the network is only decided by the links. However, in our experiments, the capacity at the bottleneck is also affected by the pedestrian density within the nodes. To be specific, as is shown in Figure 3(b), the flow rate at Q_{out} is also affected by the pedestrian density ρ within Region III. Therefore, an improved calculation method that considers the $\rho - Q_{\text{out}}$ relation in Region III should be developed to reproduce the influence of obstacle layout on egress time.

Three assumptions for calculation

In order to reproduce the $\rho - Q_{\text{out}}$ relation in Region III, we would like to consider pedestrian egress as a dynamic process rather than static. Main parameters such as Q_{obs}, Q_{out} and ρ would be time-dependent in our calculation, which means they would change with time. Based on the variation of Q_{obs} and Q_{out} with obstacle layout in Figure 3, we have listed three assumptions for the convenience of calculation.

Assumption 1: At a certain timing t, the pedestrian density $\rho(t)$ at Region III would be time–dependent that would be affected by the variation of $Q_{obs}(t)$ and $Q_{\text{out}}(t)$.

For better illustration, we assume the area of Region III as S, which is equal to the product of the obstacle-exit distance d and corridor width 3 m. Meanwhile, the density in Region III can be calculated as $\rho(t) = N_3(t)/S$. The relations among $N_3(t)$, $Q_{\text{obs}}(t)$ and $Q_{\text{out}}(t)$ can be seen in Equation 5.

$$N_3(t) = \int_0^t (Q_{obs}(x) - Q_{\text{out}}(x))\,dx \tag{5}$$

Assumption 2: when $\rho(t) < \rho_{cri}$, $Q_{\text{obs}}(t)$ equal to $Q_{\text{out}}^{\max}$ in Equation 3. When $\rho(t) \geq \rho_{cri}$, the $Q_{\text{out}}(t)$ would be equal to the $Q_{\text{out}}(t)$.

When $\rho(t) < \rho_{cri}$, the obstacle acts as the main bottleneck, making the obstacle width the contributing factor to the $Q_{\text{obs}}(t)$. In this condition, we assume the value of $Q_{\text{obs}}(t)$ is equal to $Q_{\text{obs}}^{\max}$ in Equation 3, which means $Q_{\text{obs}}(t)$ is only affected by obstacle width w. When $\rho(t) \geq \rho_{cri}$, the capacity of Region III is reached, making the exit the main bottleneck and the value of $Q_{\text{obs}}(t)$ the same with $Q_{\text{out}}(t)$.

Assumption 3: $Q_{\text{out}}(t)$ would increase with the rise of $\rho(t)$ when $\rho(t) < \rho_{cri}$, while keep constant when $\rho(t) \geq \rho_{cri}$.

We presume the relation between $Q_{\text{out}}(t)$ and $\rho(t)$ in our model is the same with the experimental results in Equation 4. Please note that Q_{out} and ρ in in Equation 4 is respectively the average exit flow rate and density during the whole process. Nevertheless, we assume that the variation trend also fits when the $Q_{\text{out}}(t)$ and $\rho(t)$ are time–dependent. To be specific, when $\rho(t) < \rho_{cri}$, the critical density in Region III is not reached. As a result, Q_{out} would gradually increase with the rise of $\rho(t)$ until the ρ_{cri} is reached. When $\rho(t) \geq \rho_{cri}$, the critical density in Region III is reached. As a result, pedestrians would keep the maximum outflow $Q_{\text{out}}^{\max}$ at the exit.

Calculation of Egress time

According to the different status of $Q_{\text{obs}}(t)$, $Q_{\text{out}}(t)$ and $\rho(t)$ in Region III, we have divided the whole egress process into four processes as shown in Table 3. The total egress time T is the accumulation of the four duration (See Equation 6). Assuming the total number of pedestrians as $N_1(0) = 49$, the egress process is terminated when the 46$^{\text{th}}$ pedestrian pass through the exit, which is in accordance with the calculation of egress time in experiments.

$$T = T_1 + T_2 + T_3 + T_4 \tag{6}$$

TABLE 3 Four processes of the egress process.

Duration	$Q_{\text{obs}}(t)$	Q_{out}	$\rho(t)$	Description
T_1	≥ 0	$= 0$	$< \rho_{cri}$	From the beginning to when the first pedestrian pass the exit.
T_2	> 0	> 0	$< \rho_{cri}$	From $Q_{\text{out}} > 0$ to when $\rho(t) = \rho_{cri}$ or to when $Q_{\text{obs}}(t) = 0$.
T_3	> 0	> 0	$= \rho_{cri}$	The duration when $\rho(t) = \rho_{cri}$ is kept.
T_4	$= 0$	≥ 0	$< \rho_{cri}$	From when $\rho(t) < \rho_{cri}$ and $Q_{\text{obs}}(t) = 0$ to when $t \geq t_{46}^{out}$.

The duration of the four processes in Table 3 could be calculated by the relations among $Q_{\text{obs}}(t)$, $\rho(t)$ and $Q_{\text{out}}(t)$ in our three assumptions. Detailed explanation of the four processes and the calculation of T_1, T_2, T_3 and T_4 are as follows. Please note that the t in the following calculation only counts from the beginning of the corresponding period, which means $t = 0$ at a certain period indicates the beginning of that period.

Calculation of T_1

In the first period, the duration is from the beginning to when the first pedestrian passes the exit. In this period, $Q_{\text{obs}}(t)$ becomes nonzero when the first pedestrian enters into Region III and $Q_{\text{out}}(t)$ is always zero. Considering that the first pedestrian is not obstructed by any other pedestrians and could walk at his desired speed, we define the duration T_1 as the time for the first pedestrian to egress from the corridor. Again, we presume the free flow velocity as $v = 1.5$ m/s and the walking distance as 8 m, and ignore the detour distance caused by the obstacle. Therefore, T_1 can be calculated in Equation 7.

$$T_1 = \frac{8\text{m}}{1.5\text{m/s}} = 6.3\text{s}. \tag{7}$$

Besides, we define the duration between the first pedestrian arrives at Region III to the first pedestrian leaves Region III as Δt, which could be calculated as $\Delta t = d/v$. During the period of Δt, $Q_{\text{obs}}(t) > 0$ while $Q_{\text{out}}(t) = 0$.

Calculation of T_2

In the second period, both the inflow and outflow exist in Region III, i.e. $Q_{\text{obs}} > 0$ and $Q_{\text{out}} > 0$. Considering the bottleneck width at the obstacle is always larger than the exit width, the inflow Q_{obs} is always higher than the outflow Q_{out}. As a result, Q_{out} and $\rho(t)$ would gradually increase. During this process, according to **Assumption 2**, the inflow should be constant as $Q_{\text{obs}}^{\max}$ that is not related to time t in this period. Nevertheless, the outflow $Q_{\text{out}}(t)$ should be time-dependent due to the variation of $\rho(t)$.

This period will terminate only if one of the two following conditions is satisfied.

Condition ①: when all the pedestrians, i.e. $N_1(0) = 49$ P, have passed by the obstacle. At the end of this period, the $Q_{\text{obs}}(T_2) = 0$ and $\rho(T_2) < \rho_{\text{cri}}$.

Condition ②: the critical density in Region III is reached. At the end of this period, the $\rho(T_2) = \rho_{\text{cri}}$ and $Q_{\text{obs}}(T_2) > 0$.

We would like to calculate T_2 through considering the two conditions. If this period is terminated by Condition ①, we assume the duration as T_2^1. If this period is terminated by Condition ②, we assume the duration as T_2^2. The relation among T_2 would equal to the smaller one between T_2^1 and T_2^2 as shown in Equation 8.

$$T_2 = \min(T_2^1, T_2^2) \tag{8}$$

In Condition ①, the duration is only decided by total pedestrian number and the flow rate at the obstacle. Therefore, T_2^1 can be calculated by Equation 9.

$$T_2^1 = \frac{N_1(0)}{Q_{\text{obs}}^{\max}} \tag{9}$$

In Condition ②, the duration is affected by time-dependent parameters including $N_3(t)$, $Q_{\text{out}}(t)$ and $\rho(t)$. According to the relations among the parameters in our three assumptions, we have listed Equation 10–11 whose solution is the duration T_2^2.

$$N_3(t) = \int_0^{\Delta t+t} Q_{\text{obs}}(x)\,dx - \int_0^t Q_{\text{out}}(x)\,dx \quad (Q_{\text{obs}}(t) = Q_{\text{obs}}^{\max}) \tag{10}$$

$$Q_{\text{out}}(t) = C\rho(t) + D = \frac{CN_3(t)}{S} + D = Q_{\text{out}}^{\max} \tag{11}$$

Equation 10 shows the pedestrian number at Region III, i.e. $N_3(t)$, which is the difference between the accumulated inflow and outflow. Equation 11 shows the relation between $N_3(t)$ and Q_{out} based on the $\rho - Q_{\text{out}}(t)$ relation shown in Equation 4. To solve Equation 10–11, we first represent $N_3(t)$ with $Q_{\text{out}}(t)$ according to Equation 11. Afterwards, the $N_3(t)$ in Equation 10 could be replaced by a formula of $Q_{\text{out}}(t)$, making Equation 10 becomes an implicit function equation of $Q_{\text{out}}(t)$ as shown in Equation 12.

$$\frac{S}{C}(Q_{\text{out}}(t) - D) = \int_0^{\Delta t+t} Q_{\text{obs}}(x)\,dx - \int_0^t Q_{\text{out}}(x)\,dx \quad (Q_{\text{obs}}(t) = Q_{\text{obs}}^{\max}) \tag{12}$$

T_2^2 can be obtained through solving Equation 12, and the solution is shown in Equation 13. Substituting T_2^1 in Equation 9 and T_2^2 in Equation 13, the value of T_2 can be illustrated in Equation 14.

$$T_2^2 = -\frac{S}{C}\ln\left(\frac{Q_{\text{out}}^{\max} - Q_{\text{obs}}^{\max}}{\left(\frac{C}{S}\Delta t - 1\right)Q_{\text{obs}}^{\max} + D}\right) \tag{13}$$

$$\begin{aligned} T_2 &= \min(T_2^1, T_2^2) \\ &= \min\left(\frac{N_1(0)}{Q_{\text{obs}}^{\max}}, -\frac{S}{C}\ln\left(\frac{Q_{\text{out}}^{\max} - Q_{\text{obs}}^{\max}}{\left(\frac{C}{S}\Delta t - 1\right)Q_{\text{obs}}^{\max} + D}\right)\right) \end{aligned} \tag{14}$$

For further calculation of T_3 and T_4, we assume the number of pedestrians that have passed by the obstale as N_{left}, and the number of pedestrians that remain in Region III at the end of this period as N_{remain}.

In the case of N_{left}, considering the inflow Q_{obs} into Region III is always constant in this period, N_{left} can be calculated by the Equation 15.

$$N_{\text{left}} = \int_0^{\Delta t + t} Q_{\text{obs}}(x)\,dx = Q_{\text{obs}}^{\max}(\Delta t + T_2) \tag{15}$$

In the case of N_{remain}, calculation of N_{remain} are different under Condition ① and Condition ②. Under Condition ①, the critical density in Region III is not reached. In this condition, $N_{\text{remain}} = N_3(T_2^1)$, which can be calculated through substituting T_2^1 into Equation 10. Under Condition ②, the critical density in Region III is reached, which means $N_{\text{remain}} = \rho_{\text{cri}}S$. Accordingly, the value of N_{remain} can be derived as shown in Equation 16.

$$N_{\text{remain}} = \begin{cases} Q_{\text{obs}}^{\max}\Delta t + (\Delta t + \dfrac{S}{C}(D - Q_{\text{obs}}^{\max}))(\exp(-\dfrac{C}{S}T_2^1) - 1) & (\rho(T_2) < \rho_{\text{cri}}) \\ \rho_{\text{cri}}S & (\rho(T_2) = \rho_{\text{cri}}) \end{cases} \tag{16}$$

Calculation of T_3

If the critical density in Region III could not be reached in the second period, i.e. $\rho(T_2) < \rho_{\text{cri}}$, the third period will not exist according to its definition. In this condition, $T_3 = 0$. If $T_3 \neq 0$, it means that $\rho(T_2) = \rho_{\text{cri}}$ and $N_{\text{remain}} = \rho \text{cri} S$ at the end of the second period. Meanwhile, the critical density in Region III will be reached, and the third period is defined as the duration that the critical density is always reached in Region III. In other words, the relation $\rho(t) = \rho_{\text{cri}}$ and $Q_{\text{out}}(t)$=$Q_{\text{obs}}(t) = Q_{\text{out}}^{\max}$ should always be satisfied. Besides, the $N_3(t)$ would always be equal to N_{left} in this period.

The third period will terminate only when all the pedestrians, i.e. $N_1(0) = 49$ P, have passed by the obstacle. With a constant outflow, T_3 can be calculated through using Q_{obs} to divide the number of pedestrians that will pass by the obstacle in this period. To all the 49 pedestrians, according to Equation 15, N_{left} pedestrians have passed by the obstacle within the first and second period, and the rest pedestrians will pass by the obstacle within the third period. Therefore, T_3 could be calculated in Equation 17.

$$T_3 = \begin{cases} 0 & (\rho(T_2) < \rho_{\text{cri}}) \\ \dfrac{N_1(0) - N_{\text{left}}}{Q_{\text{out}}^{\max}} & (\rho(T_2) = \rho_{\text{cri}}) \end{cases} \tag{17}$$

Calculation of T_4

During the fourth period, no pedestrian would step into Region III, i.e. $Q_{obs}(t) = 0$ and the initial number of pedestrians at the beginning of this period is N_{remain}. Besides, as has been mentioned before, we will stop record the time when the 46_{th} pedestrian pass the exit, which means the calculation will stop when there are three pedestrians remaining in the corridor. For calculation, we assume the time for N_{remain} pedestrians to leave Region III as T_4^1 and the time for the last three pedestrians to leave as T_4^2. The duration T_4 could be calculated by subtracting T_4^2 from T_4^1. The value of T_4^1 can be obtained by solving Equation 18–19.

$$N_3(t) = \int_0^t Q_{\text{out}}(x)\,dx = N_{\text{remain}} \tag{18}$$

$$Q_{\text{out}}(t) = C\rho(t) + D = \frac{CN_3(t)}{S} + D \tag{19}$$

Through calculating the Equation 18–19 in a way similar to the calculation of T_2^2 in Equation 10–11, the value of T_4^1, T_4^2 and T_4 could be calculated as shown in Equation 20–22.

$$T_4^1 = -\frac{S}{c}\ln\left(\frac{Q_{\text{out}}^{\max}}{\frac{C}{S}N_{\text{remain}} + D}\right) \tag{20}$$

$$T_4^2 = -\frac{S}{c}\ln\left(\frac{Q_{\text{out}}^{\max}}{3\frac{C}{S} + D}\right) \tag{21}$$

$$\begin{aligned} T_4 &= T_4^1 - T_4^2 \\ &= -\frac{S}{c}\ln\left(\frac{3C + DS}{CN_{\text{remain}} + DS}\right) \end{aligned} \tag{22}$$

According to Equation 7, 14, 17 and 22, the values of T_1, T_2, T_3 and T_4 could be obtained, and the total egress time T could be calculated based on Equation 6. Except for the constant parameters including A, B, C, D, $Q_{\text{out}}^{\max}$ and ρ_{cri}, the only two variable parameters that would affect T are S and $Q_{\text{obs}}^{\max}$, which are respectively decided by d and w. Therefore, given a certain w and d, the total egress time could be estimated.

MODELING OF EXPERIMENTAL RESULTS

Based on our mathematical model, we could estimate the egress time T under different values of w and d in order to reproduce the influence of obstacle size on egress time. To validate the model, we would like to compare the results of experiments and modeling. The obstacle layouts in our experimental settings can be seen in Table 2.

The comparison results can be seen in Figure 4. The horizontal axis represents the egress time T in our experiments and the vertical axis represents the T estimated by our model. The circular and triangle points respectively represent the T when $d = 4$ m and $d = 1$ m. The closer these points are to the $y = x$ axis, the higher the modeling accuracy is. It can be seen in Figure 4 that most data points fall into the 95% CI (confidence interval). Therefore, we presume our model is capable to reproduce the experimental egress time T.

After validating our model, we would like to calculate a more general relation between obstacle layouts, i.e. d and w, and egress time T. Compared with our experimental settings, we would like to extend the range of d to 1 m$\sim$4 m and the range of w to 0.1 m$\sim$2.0 m. The calculation results of T under different w and d could be seen in Figure 5. To help with our explanation, we have provided a three–dimensional version in Figure 5(a) and a two–dimensional version in Figure 5(b). The color bar is used to indicate the egress time T.

It can be seen in Figure 5(a) that T tends to increase with the rise of both w and d, which means both the increase of w and d would induce a longer egress time. To be specific, the increasing trend of egress time with obstacle size w is affected by the obstacle-exit distance d. When d is small, $d = 1$ m for instance, the increasing trend of T with w is relatively gentle. When d is large,

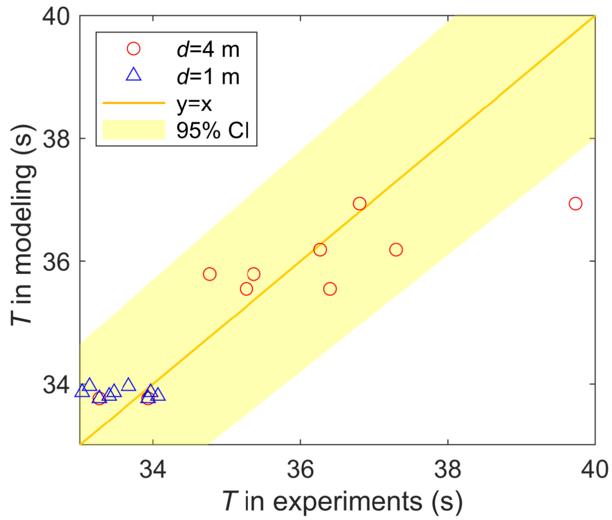

FIGURE 4 Comparison of egress time T obtained from experiments and modeling

$d = 6$ m for instance, the increasing trend of T with w is much more apparent. Therefore, it can be indicated that the larger obstacle-exit distance is, the more apparent the increasing trend of egress time is with obstacle size.

We presume the influence of obstacle-exit distance is caused to the relation between pedestrian density and exit flow rate, i.e. $\rho - Q_{\text{out}}$ relation. Compared with a larger obstacle-exit distance, a smaller obstacle-exit distance would make the area before the exit being filled quicker, thus causing a longer duration during which the exit flow rate keeps to be the maximum.

Our presumption about the increasing trend of T is in accordance with our experimental results. In our experiments, when $d = 1$ m, the increasing trend of T with w is not apparent, and the increasing trend could be fitted by a horizontal line. When $d = 4$ m, the increasing trend of T with w is more apparent and can be fitted by a linear function that rises with w.

To further evaluate whether the increasing trend is apparent or not, we have provided a two–dimensional version in Figure 5(b). Additionally, we have depicted a critical curve which indicates the critical $d - w$ relation curve illustrated by the red critical curve in Figure 5(b). When the combination (w,d) is below the critical curve, the egress time is considered to be unapparent increased. According to our experimental results, the egress time is always the least when there is no obstacle with the average value being $T^{\text{min}} = 33.6$ s. We presume that the $T(w,d)$ is not apparently different from T^{min} within a fluctuation of 5%, which can be seen in Equation 23.

$$\frac{T(w,d) - T^{\text{min}}}{T^{\text{min}}} \leq 5\% \tag{23}$$

The critical curve could be fit by a quadratic polynomial function and the reasonable combinations of w and d can be seen in Equation 24.

$$d \leq -0.40 * w^2 - 0.25 * w + 4.04 \tag{24}$$

Results in Figure 5 and Equation 24 could help guide the setting of real obstacle in engi-

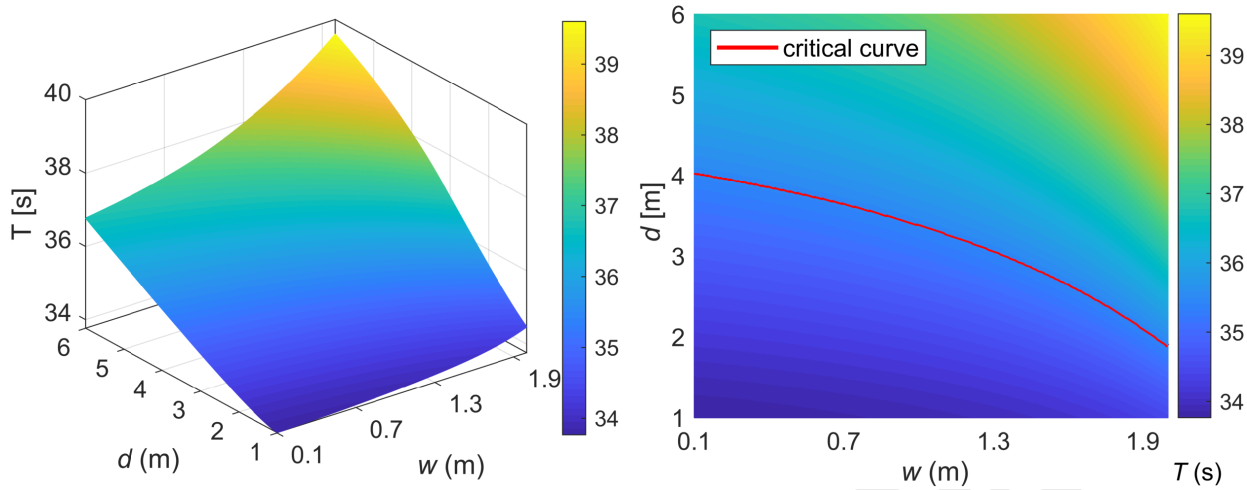

(a) Three–dimensional version (b) Two–dimensional version

FIGURE 5 Calculation results for the variation of egress time under different obstacle size w **and obstacle-exit distance** d

neering application. For instance, in the actual design of walking facilities, the obstacle would not apparently increase the egress time only if the obstacle-exit distance and obstacle size could meet the reasonable range. Nevertheless, the calculation results are affected by the constant parameters including A, B, C, D, $Q_{\text{out}}^{\max}$ and ρ_{cri}. In our model, all of the constant parameters are obtained from experimental data. It is a problem whether these constant parameters are still suitable when the geometrical size of the walking scenario is largely different from our experiments.

CONCLUSION AND DISCUSSION

In this study, we have conducted both experimental and mathematical modeling methods to explore the influence of obstacle on the egress time of pedestrians in normal conditions. In our experiments, we built a corridor with a wall–shaped obstacle in the middle, and changed the obstacle size and obstacle-exit distance to explore the corresponding influence. Results show that the influence of obstacle size on egress time is affected by the obstacle-exit distance. When the obstacle-exit distance is small, the obstacle size has no apparent influence on the egress time. However, when the obstacle-exit distance is large, the egress time would roughly increase with the obstacle size.

We presume the influence of obstacle-exit distance can be explained through abstracting the walking scenarios into a simple network and exploring the function of obstacle as a bottleneck. When the obstacle is near to the exit, the flow rate at obstacle bottleneck is not affected by obstacle size. In this situation, the obstacle bottleneck is an ‘ineffective’ bottleneck that would guide pedestrians other than obstructing them. When the obstacle is far from the exit, the flow rate at the obstacle bottleneck would decrease with the increase of obstacle size. In this situation, the obstacle bottleneck is an ‘effective’ bottleneck that would reduce the egress time through impeding pedestrian movement.

It is interesting that in our experiments, the flow rate at the exit is always the least while the exit is not always the ‘effective’ bottleneck. However, in traditional calculation methods of network, the ‘effective’ bottleneck should be the one with the least flow rate. In consequence, the traditional methods cannot reproduce the influence of obstacle layout on the egress time.

To further explore the influencing mechanism of obstacle layout behind the experimental data, we have built a mathematical model that can reproduce the influence of obstacle layout on egress time in our experiments. Moreover, the model can estimate the egress time under a wider range of obstacle width and obstacle-exit distance. As a result, the reasonable combinations of obstacle size and obstacle-exit distance that would not apparently increase the egress time have been obtained.

Results in this study are expected to help with the actual design of obstacle in walking facilities. For instance, the obstacle in actual walking facilities should not apparently affect the egress time. Our modeling results could help evaluate whether a certain obstacle layout is under the reasonable range and provide feasible schemes to improve the obstacle layout. Nevertheless, there are also some limitations in our mathematical model. The constant parameters for modeling might change under geometrical settings of the walking scenario. For practical use, these constant parameters should be measured in the actual design of obstacle in walking facilities. As our future work, we would like to explore the variation of the constant parameters with the change of geometrical sizes of the walking scenario, thus extending our mathematical model for a higher application value. In consequence, we expect to help verify and improve the obstacle design rules in the present design criterion of walking facilities with the extended model in the future.

ACKNOWLEDGEMENTS

This work was partially supported by JST-Mirai Program Grant Number JPMJMI17D4, Japan and MEXT as "Priority Issues and Exploratory Challenges on post-K (Supercomputer Fugaku)" (Exploratory Challenge 2: Construction of Models for Interaction Among Multiple Socioeconomic Phenomena, Model Development and its Applications for Enabling Robust and Optimized Social Transportation Systems) (Project ID: hp190163).

REFERENCES

1. Kirchner, A., K. Nishinari, and A. Schadschneider, Friction effects and clogging in a cellular automaton model for pedestrian dynamics. *Phys. Rev. E*, Vol. 67, 2003, p. 056122.
2. Zuriguel, I., A. Janda, A. Garcimartín, C. Lozano, R. Arévalo, and D. Maza, Silo Clogging Reduction by the Presence of an Obstacle. *Phys. Rev. Lett.*, Vol. 107, 2011, p. 278001.
3. Zuriguel, I., J. Olivares, J. M. Pastor, C. Martín-Gómez, L. M. Ferrer, J. J. Ramos, and A. Garcimartín, Effect of obstacle position in the flow of sheep through a narrow door. *Phys. Rev. E*, Vol. 94, 2016, p. 032302.
4. Shiwakoti, N. and M. Sarvi, Enhancing the panic escape of crowd through architectural design. *Transportation Research Part C: Emerging Technologies*, Vol. 37, 2013, pp. 260 – 267.
5. Lin, P., J. Ma, T. Y. Liu, T. Ran, Y. L. Si, F. Y. Wu, and G. Y. Wang, An experimental study of the impact of an obstacle on the escape efficiency by using mice under high competition. *Physica A: Statistical Mechanics and its Applications*, Vol. 482, 2017, pp. 228 – 242.
6. Duives, D. C., W. Daamen, and S. P. Hoogendoorn, State-of-the-art crowd motion simulation models. *Transportation Research Part C: Emerging Technologies*, Vol. 37, 2013, pp. 193 – 209.
7. Yanagisawa, D., A. Kimura, A. Tomoeda, R. Nishi, Y. Suma, K. Ohtsuka, and K. Nishinari, Introduction of frictional and turning function for pedestrian outflow with an obstacle. *Phys. Rev. E*, Vol. 80, 2009, p. 036110.
8. Yanagisawa, D., R. Nishi, A. Tomoeda, K. Ohtsuka, A. Kimura, Y. Suma, and K. Nishinari, Study on Efficiency of Evacuation with an Obstacle on Hexagonal Cell Space. *SICE Journal of Control, Measurement, and System Integration*, Vol. 3, No. 6, 2010, pp. 395–401.
9. Zhao, Y., M. Li, X. Lu, L. Tian, Z. Yu, K. Huang, Y. Wang, and T. Li, Optimal layout design of obstacles for panic evacuation using differential evolution. *Physica A: Statistical Mechanics and its Applications*, Vol. 465, 2017, pp. 175 – 194.
10. Frank, G. and C. Dorso, Room evacuation in the presence of an obstacle. *Physica A: Statistical Mechanics and its Applications*, Vol. 390, No. 11, 2011, pp. 2135 – 2145.
11. Shiwakoti, N., X. Shi, and Z. Ye, A review on the performance of an obstacle near an exit on pedestrian crowd evacuation. *Safety Science*, Vol. 113, 2019, pp. 54 – 67.
12. Shiwakoti, N., M. Sarvi, G. Rose, and M. Burd, Consequence of Turning Movements in Pedestrian Crowds during Emergency Egress. *Transportation Research Record*, Vol. 2234, No. 1, 2011, pp. 97–104.
13. Karbovskii, V., O. Severiukhina, I. Derevitskii, D. Voloshin, A. Presbitero, and M. Lees, The impact of different obstacles on crowd dynamics. *Journal of Computational Science*, 2018.
14. Li, J., L. Jingyu, S. Chao, Y. Sicong, and Z. Han, Obstacle optimization for panic flow reducing the tangential momentum increases the escape speed. *Plos One*, Vol. 9, 2014, pp. 1 – 15.
15. Cristiani, E. and D. Peri, Robust design optimization for egressing pedestrians in unknown environments. *Applied Mathematical Modelling*, Vol. 72, 2019, pp. 553 – 568.
16. Rudloff, C., T. Matyus, S. Seer, and D. Bauer, Can Walking Behavior be Predicted?: Analysis of Calibration and Fit of Pedestrian Models. *Transportation Research Record*, Vol. 2264, No. 1, 2011, pp. 101–109.

17. Parisi, D. R., P. A. Negri, and L. Bruno, Experimental characterization of collision avoidance in pedestrian dynamics. *Phys. Rev. E*, Vol. 94, 2016, p. 022318.
18. Jia, X., C. Feliciani, D. Yanagisawa, and K. Nishinari, Experimental study on the evading behavior of individual pedestrians when confronting with an obstacle in a corridor. *Physica A: Statistical Mechanics and its Applications*, Vol. 531, 2019, p. 121735.
19. Shi, X., Z. Ye, N. Shiwakoti, D. Tang, and J. Lin, Examining effect of architectural adjustment on pedestrian crowd flow at bottleneck. *Physica A: Statistical Mechanics and its Applications*, Vol. 522, 2019, pp. 350 – 364.
20. Lian, L., X. Mai, W. Song, Y. K. K. Richard, X. Wei, and J. Ma, An experimental study on four-directional intersecting pedestrian flows. *Journal of Statistical Mechanics: Theory and Experiment*, Vol. 2015, No. 8, 2015, p. P08024.
21. Garcimartín, A., D. Maza, J. M. Pastor, D. R. Parisi, C. Martín-Gómez, and I. Zuriguel, Redefining the role of obstacles in pedestrian evacuation. *New Journal of Physics*, Vol. 20, No. 12, 2018, p. 123025.
22. Hoogendoorn, S. P. and W. Daamen, Pedestrian Behavior at Bottlenecks. *Transportation Science*, Vol. 39, No. 2, 2005, pp. 147–159.
23. Daamen, W., S. P. Hoogendoorn, and P. H. L. Bovy, First-Order Pedestrian Traffic Flow Theory. *Transportation Research Record*, Vol. 1934, No. 1, 2005, pp. 43–52.
24. Hoogendoorn, S. P. and W. Daamen, Pedestrian Behavior at Bottlenecks. *Transportation Science*, Vol. 39, No. 2, 2005, pp. 147–159.
25. Shahhoseini, Z., M. Sarvi, M. Saberi, and M. Haghani, Pedestrian Crowd Dynamics Observed at Merging Sections: Impact of Designs on Movement Efficiency. *Transportation Research Record*, Vol. 2622, No. 1, 2017, pp. 48–57.
26. Qiu, G., R. Song, S. He, and W. Yin, The pedestrian flow characteristics of Y-shaped channel. *Physica A: Statistical Mechanics and its Applications*, Vol. 508, 2018, pp. 199 – 212.
27. Ezaki, T., D. Yanagisawa, and K. Nishinari, Pedestrian flow through multiple bottlenecks. *Phys. Rev. E*, Vol. 86, 2012, p. 026118.
28. Chattaraj, U., A. Seyfried, and P. Chakroborty, Comparison of pedestrian fundamental diagram across cultures. *Advances in Complex Systems*, Vol. 12, No. 03, 2009, pp. 393–405.
29. Boltes, M. and A. Seyfried, Collecting pedestrian trajectories. *Neurocomputing*, Vol. 100, 2013, pp. 127 – 133, special issue: Behaviours in video.
30. Ravindra, A., K., M. Thomas, L., and O. James, B., *Network Flows: Theory, Algorithms, and Applications*, 1988.